High-cycle fatigue behavior of low-C medium-Mn high strength steel with austenite-martensite submicron-sized lath-like structure

X.Y. Qi[a], L.X. Du[a,*], J. Hu[a], R.D.K. Misra[b]

[a] The State Key Laboratory of Rolling and Automation, Northeastern University, Shenyang 110819, China
[b] Laboratory for Excellence in Advanced Steel Research, Department of Metallurgical, Materials and Biomedical Engineering, University of Texas at El Paso, TX 79968-0521, USA

A B S T R A C T

In this study, the high-cycle fatigue behavior of low-C medium-Mn high strength steel was studied at stress ratio R ($\sigma_{min}/\sigma_{max}$) = − 1 and 0.1. Excellent fatigue performance with push-pull fatigue limit strength (σ_{-1}) and pull-pull fatigue limit strength ($\sigma_{0.1}$) after 10^7 cycles of 450 MPa and 683 MPa was obtained. The fatigue ratio (σ_{-1}/R_m, $\sigma_{0.1}/R_m$) was 0.54 and 0.82, respectively. Two types of failure modes were observed, surface-induced failure mode and internal inclusion-induced failure mode. The retained austenite (RA) transformation ratio of fracture surface increased from ~ 30% to ~ 63% with increase in maximum stress (σ_{max}) from 470 MPa to 550 MPa. The higher mechanical driving force contributed to the total driving force for martensite transformation, and higher damage accumulation in terms of cyclic plasticity. The high density of high misorientation boundaries between tempered martensite effectively prevented the propagation of fatigue crack, and enhanced the fatigue strength. The experimental steel with excellent fatigue property was mainly attributed to the transformation-induced plasticity (TRIP) effect of metastable RA in the small plastic deformation zone, which relaxed the local stress concentration, absorbed the strain energy, delayed the crack initiation and suppressed its propagation.

1. Introduction

There is growing interest in medium-Mn TRIP steels because of its good combination of high strength, excellent ductility, and low-cost [1,2]. Now, the majority of studies on medium-Mn steels focus on the effect of alloying elements, thermo-mechanical controlled process (TMCP), and intercritical annealing step on the microstructure and mechanical properties [1,3–5]. For example, Aydin et al. [3] discussed the effect of alloy composition on the deformation mechanisms in medium-Mn steels. Hu et al. [4] studied the ductility and toughness of 5Mn steel. Lee et al. [5] investigated the optimal intercritical annealing temperature for medium-Mn steel. However, the study on fatigue property of medium-Mn TRIP steels has not been reported.

In general, a material that with stands up to 10^7 cycles and is not broken is defined as the high-cycle fatigue limit, which means the material has an infinite life [6]. In high-cycle fatigue scenario, the material performance is commonly characterized by S-N curve. The S-N curve is crucial for establishment of a design that is robust to fatigue failure [7].

Fatigue performance is an important material property from an engineering point of view, and the fatigue failure is one of the most serious types of failure for steel structures [8]. The fatigue limit of steel is directly proportional to its ultimate tensile strength for low strength steels [9]. But for high strength steels, the fatigue limit data is scattered. Fatigue cracks may initiate and propagate under cyclic loading if the stress level is larger than the fatigue limit [10]. The fatigue fracture stress is usually lower than the yield strength, and there is no visible plastic deformation in fatigue damage [11]. Thus, there is no indication before fatigue fracture, which may result in casualties and considerable economic loss [8]. As a result, study on the fatigue property of medium-Mn TRIP steels is significant for product design and service life.

The study focuses on the high-cycle push-pull axial loading fatigue behavior of medium-Mn TRIP steel and determines the fatigue limit. In addition, the mechanism of TRIP effect on the fatigue property is elucidated.

2. Experimental procedure

The experimental steel was produced by Anshan Iron & Steel Company. The nominal chemical composition of the steel in weight percent was 0.05C, 0.2Si, 5.0Mn, P ≤ 0.008, S ≤ 0.006, 0.4Cr, 0.16Mo, 0.31Ni, 0.15Cu, and balance Fe. The 230 mm thick slab was
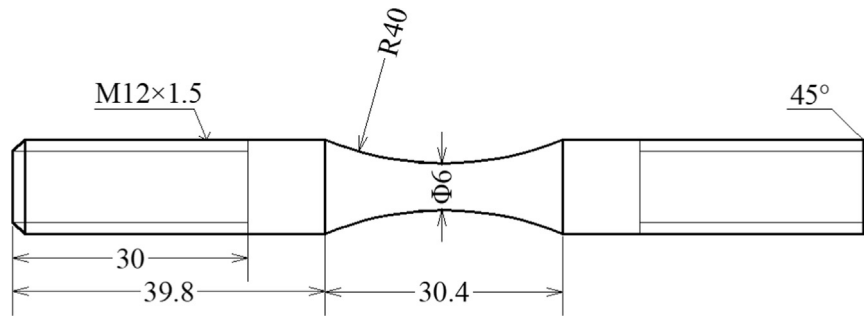
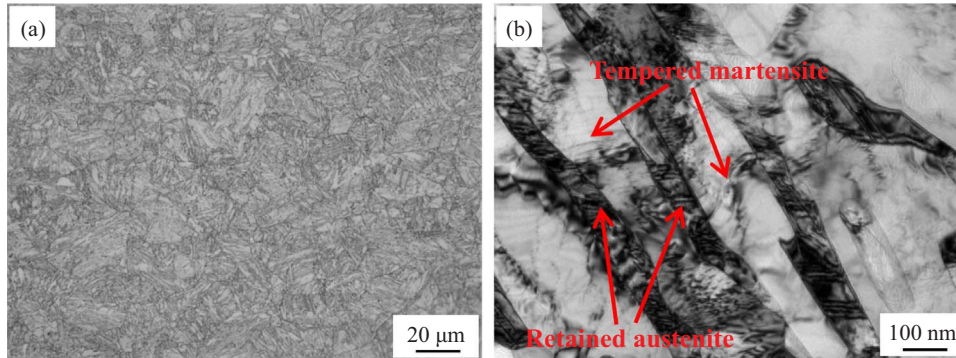**Fig. 1.** Smooth hourglass-shaped specimen for fatigue test.

Fig. 2. Microstructure of experimental steel: (a) OM, (b) TEM.

austenitized at 1180 °C and subjected to two stages of controlled-rolling. The finish rolling thickness was 30 mm. Then, the plate was directly water-quenched (DQ) to room temperature, and intercritically annealed at 630 °C for 30 min between the two phase region ($\alpha + \gamma$). Finally, the tempered martensite and RA submicron-sized lath-like microstructure was obtained.

The tensile specimens of dimensions 6 mm diameter and 25 mm length were machined from the plates parallel to the rolling direction at 1/4 thickness. Tensile tests were performed using a Shimadzu AG-X universal testing machine at room temperature with a crosshead speed of 3 mm/min according to ISO 6892-1:2009. The tensile strength data was an average of three measurements.

Fatigue specimens from the tested steel plate were machined with the longitudinal axis along the rolling direction at 1/4 thickness. The fatigue specimen diagram is shown in Fig. 1. The surface of specimens was prepared by fine grinding and final polishing, in order to eliminate the residual stress and improve the surface smoothness. The surface conditions are important for high-cycle fatigue and fatigue limit. The S-N curve of experimental steel was established by signal specimen method, and the fatigue limit was determined by up-and-down test [12,13]. The fatigue limit was calculated using the following Eq. (1):

$$\sigma_{-1} = \frac{1}{m} \sum_{i=1}^{n} \nu_i \sigma_i \qquad (1)$$

where m is the number of effective test, n is number of stress level, ν_i is the number of test under i stress level, σ_i is the i stress level. The push-pull and pull-pull axial loading fatigue test was performed on GPS-100 high-frequency testing machine at a frequency of 150 Hz up to 10^7 cycles at room temperature. Constant amplitude fatigue test was performed at a stress ratio R = − 1 and R = 0.1, respectively. Compressed air was introduced to eliminate possible "self-heating" of specimens during the test.

The microstructure of specimen was characterized using a Leica DMIRM optical microscope (OM) and Zeiss Ultra 55 scanning electron microscope (SEM) equipped with electron backscattered diffraction (EBSD) system. Fracture surface of specimens was observed by FEI

Quanta 600 SEM and FEI Tecnai G2 F20 transmission electron microscope (TEM) at an accelerating voltage of 200 kV. The volume fraction of RA of fracture surface was determined by D/max2400 X-ray diffraction (XRD) using a Cu-Kα radiation source at room temperature with the scanning speed of 2°/min. The integrated intensities of (200)γ, (220)γ, (311)γ, (200)α, and (211)α peaks was used to quantify the amount of RA using Eq. (2) [14]:

$$V_\gamma = 1.4I_\gamma/(I_\alpha + 1.4I_\gamma) \qquad (2)$$

where V_γ is the volume fraction of RA, I_γ is the integrated intensity of γ peaks, and I_α is the integrated intensity of α peaks.

3. Results

3.1. Microstructure and tensile properties

The microstructure of the experimental steel is presented in Fig. 2. Based on our previous study [15,16], the OM (Fig. 2a) and TEM (Fig. 2b) of experimental steel indicated tempered martensite and strip-shaped RA. The width of tempered martensite laths and RA was in the range of ∼ 100–450 nm and ∼ 50–100 nm, respectively. Moreover, the dislocation density of tempered martensite matrix was low.

The engineering stress-strain curve of the experimental steel is illustrated in Fig. 3. The yield strength, tensile strength (R_m), elongation after fracture, and elastic modulus (E) were 720 MPa, 830 MPa, 26.34%, and 2.06×10^5 MPa, respectively. During plastic deformation, the transformation of RA to martensite provided a localized work hardening effect, which relaxed the stress concentration, delaying the onset of necking, and increasing the uniform elongation [15,17,18]. Furthermore, the newly formed hard martensite phase enhanced tensile strength of experimental steel [18]. Thus, the experimental steel had a good combination of strength and ductility.

3.2. High-cycle fatigue behavior

The applied stress versus number of cycles to fatigue fracture or run-